

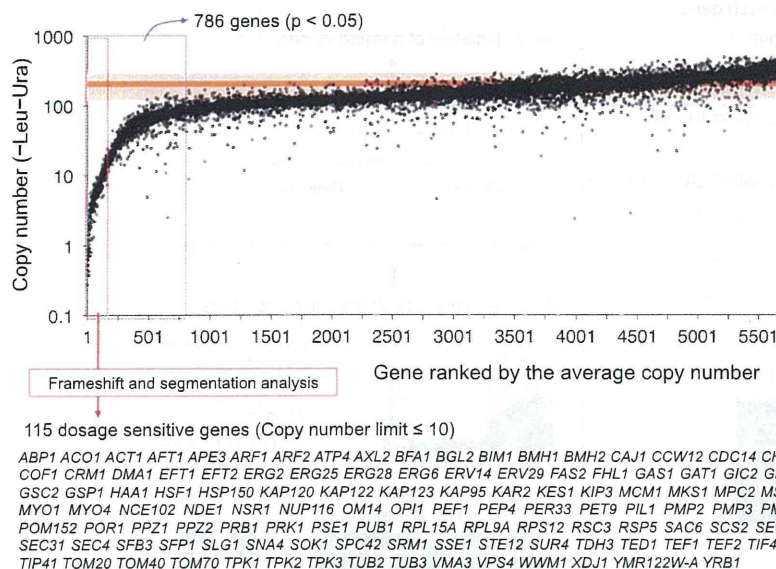
yeast genome (the entire data can be found in Supplemental Table S1). Hereafter, we will refer to this analysis as “gTOW6000.”

Figure 2 shows the copy number under the –Leu–Ura condition determined in gTOW6000. gTOW6000 was performed using 96-well microplates. We handled 244 plates, as we analyzed two clones under two culture conditions for each gene. For the purpose of data quality control and to obtain a negative control, several empty vector experiments were performed for each plate (a total of 230 measurements) (Supplemental Table S2). The average of the empty vector experiments is shown as the orange line in Figure 2. To identify genes with significantly lower limits than the empty vector control, we evaluated the copy number data under the –Leu–Ura condition using Student’s *t*-test. In total, 919 genes had *P*-values <0.05, and 786 of them had lower copy numbers than the vector average (genes surrounded by a blue-dotted rectangle in Fig. 2). We thus considered the copy numbers of these genes under the –Leu–Ura condition to be their CNLs of overexpression. The average copy number of these genes was less than 85. This finding conversely indicates that the other 5000 genes have similar or higher CNLs than the detectable CNL in gTOW using pTOWug2-836, and suggests that the yeast cellular system is generally robust against a nearly 100-fold increase in the copy number of any one of 80% of its genes. Although some genes displayed much higher limits than the vector average, there was no reproducibility between the two clones (Pearson’s correlation coefficient between the duplicates of genes with average copy numbers of >250 was –0.26). We thus concluded that the findings were reflective of experimental errors.

In gTOW, there should be a correlation between the CNLs and max growth rates of low limit genes (Moriya et al. 2006, 2012). In

addition, there should be a correlation between the copy numbers under the –Ura and –Leu–Ura conditions (Moriya et al. 2006). These expectations were confirmed in gTOW6000 (Supplemental Table S3). We next calculated the copy number causing 50% growth inhibition in gTOW6000. To reduce the effect of experimental errors, we first calculated the moving averages of max growth rates and CNLs for 100 of the 786 genes with significantly low CNLs (Supplemental Fig. S4A). To approximate the relationship between CNL and max growth rate (Supplemental Fig. S4B), we derived a first dimension equation as follows:  $CNL = 49.24 \times [\text{max growth rate}]$  ( $R^2 = 0.98$ ). From the equation, the copy number that gave 50% growth inhibition (max growth rate = 1.11) was calculated to be 54.7 copies. If the target gene has a very low limit, then the cells expressing the gTOW plasmid cannot grow under the –Leu–Ura condition because they cannot produce sufficient amounts of leucine (Moriya et al. 2006). We next evaluated the lower limit copy number resulting in no growth in gTOW6000. We calculated the moving averages of max growth rates as described previously in this section. For each bin, we then counted the number of genes displaying no growth (max growth rate is set as 0.1; see Methods) in both of the duplicated experiments (i.e., frequency of no-growth) (Supplemental Fig. S5A). To approximate the relationship between frequency of no-growth and CNL (Supplemental Fig. S5B), we derived the following equation:  $[\text{frequency of no-growth}] = -0.0002 \times CNL^3 + 0.0476 \times CNL^2 - 3.6046 \times CNL + 101.53$  ( $R^2 = 0.996$ ). We used this equation to calculate that a gene with a CNL of 18.4 could not grow in 50% of cases in the gTOW experiment.

By use of genome-wide screening, Sopko et al. (2006) previously isolated 767 *S. cerevisiae* genes that caused cellular growth defects when overexpressed by the *GAL1* promoter. As we isolated a similar number of genes with low CNLs (786 genes), we compared two data sets. As shown in Figure 3A, only 161 of the 786 genes isolated by gTOW6000 overlapped with those in the study by Sopko et al. (2006), although the overlap was significant ( $P < 1.5 \times 10^{-8}$ , chi-square test). The difference possibly arose from the difference in the experimental systems for overexpressing genes, as is discussed in the Introduction. The difference was significant when we separated isolated genes by their native expression levels (Fig. 3B). Highly expressed genes were significantly isolated as genes with low CNLs in gTOW6000 ( $P = 1.322 \times 10^{-15}$  in the Mann-Whitney *U*-test), whereas this finding was not replicated in the study by Sopko et al. (2006) ( $P = 0.7378$  in the Mann-Whitney *U*-test). Another difference between the two experiments was the proportions of protein complex members. The 786 genes isolated by gTOW contained significant numbers of protein complex members (Table 1), whereas the 767 genes isolated by Sopko et al. (2006) did not contain many protein complex members (Table 1). This might reflect the fact that protein complex members tend to be highly expressed (Supplemental



**Figure 2.** Copy number limits (CNLs) of *S. cerevisiae* genes determined by gTOW analysis. Genes were ordered according to their average copy number determined by gTOW under the –Leu–Ura condition. Each gene has two data points because of the duplication of the experiment. The orange line and the transparent zone around the line indicate the average copy number with the empty vector and the standard deviation, respectively. Genes that showed significantly lower limits than those observed in the vector experiments (786 genes,  $P < 0.05$ ) are surrounded by the blue dotted rectangle. Genes with CNLs of 10 and less (dosage-sensitive genes [DSGs]) are surrounded by the red-dotted rectangle. A confident set of DSGs isolated after frameshift and segmentation analyses (Fig. 4) is shown. The entire data set is given in Supplemental Table S1.

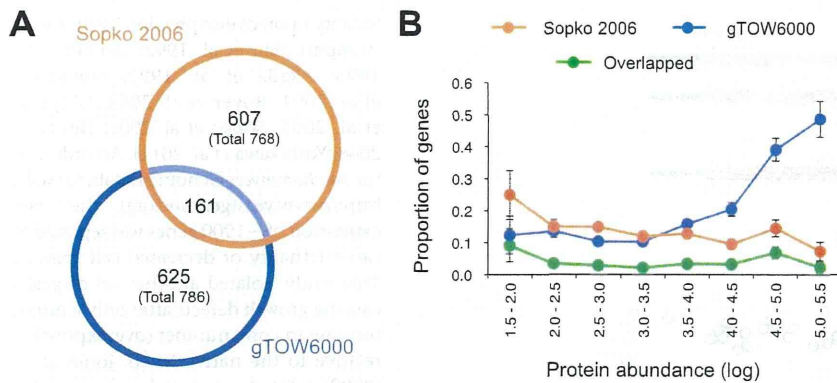


**Figure 3.** Comparison of gTOW6000 data with data of another overexpression analysis performed using promoter swapping. (A) Overlap of genes identified by the overexpression analyses performed by Sopko et al. (2006) and in this study. (B) Distribution of genes identified by overexpression analysis ordered by their native protein levels. Each bin contains genes ordered by their native protein levels (Ghaemmaghami et al. 2003). The protein abundance unit is molecules per cell. Error bars, SEM.

Fig. S6). From these results, we considered that gTOW6000 would provide additional clues to understand the cellular effects of gene overexpression, as this method isolated a different subset of genes from previous promoter swapping experiments. Of the 161 overlapped genes (Fig. 3A), the highly expressed genes among the 786 gTOW6000 genes were excluded (Fig. 3B), and the complex members of 767 genes isolated by Sopko et al. (2006) were enriched (Table 1), probably due to the characteristics of the opposite data sets.

### Isolation of low limit genes (yeast DSGs)

To further understand the characteristics of low limit genes, we performed additional experiments to isolate a confident set of genes with CNLs of 10 or less. We introduced a frameshift mutation in each of the 182 genes to confirm whether the expression of the protein but not that of the DNA and RNA elements determined the limit (Fig. 4A). Frameshift analysis could also determine whether either of the bidirectionally overlapped genes was

the cause of the low CNL (for example, see Supplemental Fig. S7A). Among the 155 genes with CNLs of 20 or less, the frameshift mutants of 140 of these genes displayed more than fivefold higher CNLs than the wild-type genes or their CNLs increased to the vector level (~100 copies) (Fig. 4B; Supplemental Table S4). We thus verified that the original target ORFs of these 140 genes determined the CNLs (denoted as “fs verified” in Supplemental Tables S1, S4).

We further analyzed the 15 genes in frameshift mutants that did not exhibit increased limits (12 of them are indicated by red circles in Fig. 4B). They were categorized as four different types of genes as follows. (1) One of the overlapping ORFs appeared to cause the low limits. The cloned regions contained two overlapping ORFs in cases of *YFL010C/WWM1-YFL010W-A/AUA1* and *YGL167C/PMR1-YGL168W/HUR1*. Because the frameshift mutants of *WWM1* and *PMR1* displayed increased CNLs, we concluded that these genes were responsible for the low CNLs. The result for *YGL167C* is shown in Supplemental Figure S7A as an example. (2) Because both clones containing one of the two neighboring genes (*YNL024C-A/KSH1-YNL025C/SSN8*) exhibited low CNLs but the frameshift mutations did not increase the CNL of either gene (Supplemental Fig. S7B), we concluded that an RNA gene (*NME1*) caused the low limits. (3) For genes for which the frameshift mutations did not increase their CNLs but the cause could not be ascertained from their genome annotations, we segmented the fragments into 5' UTR and ORF-3' UTR fragments and measured their limits (Fig. 4A). Both the 5' and 3' segmented fragments of *CPS1*, *FHL1*, *GRX3*, *HOM3*, *TPK1*, and *TPK3* (underlined in blue in Fig. 4C) displayed increased copy numbers. These ORFs may have been expressed from ATGs other than the annotated ones. (4) The segmented fragments (ORF-3' UTR) of *ASE1*, *DIE2*, *IRC8*, and *SFP1* did not exhibit increased CNLs (underlined in red, Fig. 4C). For *DIE2* and *IRC8*, we

**Table 1.** Characteristics of DSGs

	Protein complex members <sup>a</sup>	Genes with no. of PPIs ≥10 <sup>b</sup>	Genes with no. of PPIs ≥5 <sup>b</sup>	Intrinsic protein disorder (≥150) <sup>c</sup>	Yeast ohnologs <sup>d</sup>	Essential genes <sup>e</sup>
Yeast DSG <sup>f</sup> (limit ≤10)	69.6% (80/115)	75.7% (87/115)	36.5% (42/115)	23.5% (27/115)	34.8% (40/115)	26.1% (30/115)
<i>P</i> -value	$9.05 \times 10^{-7}$	$7.80 \times 10^{-10}$	$1. \times 10^{-10}$	$3.43 \times 10^{-7}$	$2.21 \times 10^{-5}$	—
gTOW6000 786 genes	61.5% (483/786)	60.3% (474/786)	25.7% (202/786)	24.8% (195/786)	27.2% (214/786)	27.4% (215/786)
<i>P</i> -value	$<2.2 \times 10^{-16}$	$9.37 \times 10^{-15}$	$<2.2 \times 10^{-16}$	$<2.2 \times 10^{-16}$	$3.23 \times 10^{-10}$	$9.90 \times 10^{-8}$
Overlapped 161 genes	62.7% (101/161)	64.6% (104/161)	29.8% (48/161)	32.3% (52/161)	34.8% (56/161)	28.0% (45/161)
<i>P</i> -value	$4.06 \times 10^{-5}$	$1.37 \times 10^{-5}$	$1.40 \times 10^{-7}$	$4.91 \times 10^{-12}$	$3.75 \times 10^{-7}$	0.01705
Sopko 767 genes	46.0% (353/767)	57.4% (440/767)	21.1% (162/767)	26.2% (201/767)	21.8% (167/767)	20.9% (160/767)
<i>P</i> -value	—	$3.92 \times 10^{-9}$	$3.08 \times 10^{-7}$	$<2.2 \times 10^{-16}$	$3.91 \times 10^{-2}$	—
All genes	46.5% (2690/5783)	47.4% (2742/5783)	14.9% (863/5783)	13.6% (786/5783)	19.0% (1098/5783)	20.2% (1168/5783)

<sup>a</sup>Protein complex components (mips; ftp://ftp.mips.gsf.de/yeast/catalogues/complexcat/complexcat\_data\_18052006).

<sup>b</sup>Protein–protein interactions (dip; http://dip.doe-mbi.ucla.edu).

<sup>c</sup>Intrinsic protein disorder (Vavouri et al. 2009).

<sup>d</sup>Yeast ohnolog (http://wolfe.gen.tcd.ie/ygob/).

<sup>e</sup>Essential genes (http://www-deletion.stanford.edu/YDPM/YDPM\_index.html).

<sup>f</sup>Complete data set for yeast DSGs is given in Supplemental Table S5.

Makanae et al.

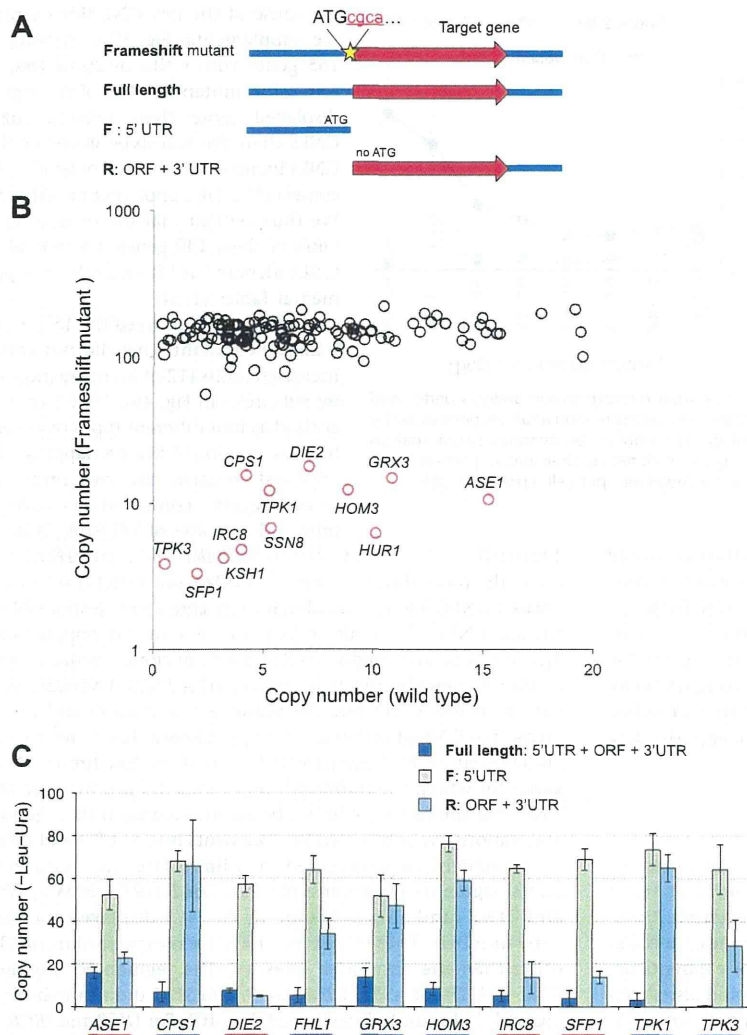


**Figure 4.** Frameshift and segmentation analyses of candidate low limit genes. (A) Structure of the plasmid used in frameshift analysis and segmentation analysis. (Red letters) The nucleotide inserted to generate frameshift. The introduced FspI site in the mutant is underlined. (B) A scatter plot of the CNLs of the wild-type genes and the frameshift mutants of low limit genes. (Black circles) Genes that displayed increased CNLs when frameshift was introduced. (Red circles) Genes that did not display increased CNLs even when frameshift was generated. Note that the frameshift mutants of *AUA1*, *GAT1*, and *FHL1* could not be obtained, probably because their frameshift mutants also have very low limits. The raw data can be found in Supplemental Table S4. (C) CNLs of segmented genes. Genes underlined with a blue line are those that displayed increased CNLs upon segmentation. Genes underlined with a red line indicate genes that did not display increased CNLs upon segmentation.

performed additional segmentation analysis (Supplemental Fig. S8). The 3' regions of both genes had elements causing the low limits, although their functions are still unknown (Supplemental Fig. S8).

By use of the aforementioned analysis, we isolated 115 DSGs by removing the overlapping genes (*AUA1* and *HUR1*), the RNA gene (*NME1*), the genes for which their low limits were not caused by their annotated ORFs (*DIE2* and *IRC8*), and a real-time PCR reference gene (*LEU3*) from the list of genes with CNLs of 10 or less (Fig. 2; Supplemental Table S5). Among the yeast DSGs, 88 genes were previously isolated in screenings of genes causing

toxicity upon overexpression by promoter swapping (Liu et al. 1992; Espinet et al. 1995; Akada et al. 1997; Stevenson et al. 2001; Boyer et al. 2004; Gelperin et al. 2005; Sopko et al. 2006; Niu et al. 2008; Yoshikawa et al. 2011). According to the *Saccharomyces* Genome Database (SGD; <http://www.yeastgenome.org>), the overexpression of ~1900 genes was reported to cause lethality or decreased cell growth. This study isolated another set of genes causing growth defects after only a minor increase in copy number (overexpression relative to the native level). Jones et al. (2008) created a comprehensive overlap DNA library of the *S. cerevisiae* genome using a 2-micron-based multicopy vector. They tested the toxicity of each clone to yeast cells and identified 23 toxic DNA segments. We can assume that the yeast DSGs isolated in our study are responsible for the toxicity of the DNA segments. In total, 12 of the 23 toxic clones actually contained DSGs isolated in this study (Supplemental Table S6). At present, it is unclear why clones without yeast DSGs are toxic. The toxicities of these clones might be explained by the additive effect of weak DSGs within the same clone, or we may have failed to clone the promoters of target genes that were present beyond the neighboring genes.

We next analyzed the characteristics of isolated DSGs (Table 1). DSGs significantly contain protein complex members, proteins with many interaction partners, and proteins containing higher intrinsic disordered regions. Although it was not significant, the percentage of essential genes among yeast DSGs was higher than that within the entire genome. DSGs also tended to be highly expressed ( $P = 4.696 \times 10^{-6}$  in the Mann-Whitney *U*-test) (Supplemental Fig. S9), as did the 786 low limit genes (Fig. 3B). Yeast DSGs contain significantly higher percentages of genes in the gene ontology categories of cytoskeletal organization and intracellular transport (Table 2), whereas transcription factors and signaling molecules (protein kinase and phosphatase) were not concentrated (data not shown). Figure 5 presents a gene network constituted according to the functional category of each gene and their physical (protein-protein and protein-DNA) interactions that were described in SGD.

#### Protein burden causes dosage sensitivity

The fact that DSGs tended to be highly expressed suggests that the increased copy number of a highly expressed gene exerts a burden on protein turnover (Stoebel et al. 2008; Sheltzer and Amon 2011), which causes the dosage sensitivities of yeast DSGs. We thus se-

**Table 2.** Gene Ontology analysis of yeast DSGs

	Gene Ontology identification: term	Observation	Mean	SD	Z-score	P-value
Biological process	0006810: Transport	41	25.1	4.2	3.8	$1.37 \times 10^{-2}$
	0016044: Cellular membrane organization	17	6.8	2.4	4.2	$1.38 \times 10^{-2}$
	0007049: Cell cycle	25	12.8	3.4	3.6	$2.19 \times 10^{-2}$
	0016192: Vesicle-mediated transport	20	9.2	2.8	3.9	$2.25 \times 10^{-2}$
Molecular function	N.A.					
Cellular component	0005856: Cytoskeleton	19	4.9	2.2	6.3	$5.49 \times 10^{-6}$
	0005938: Cell cortex	12	3.4	1.7	4.9	$2.55 \times 10^{-3}$
	0005624: Membrane fraction	13	4.6	2	4.3	$1.24 \times 10^{-2}$
	0030427: Site of polarized growth	14	5.4	2.2	3.9	$1.52 \times 10^{-2}$
	0016023: Cytoplasmic membrane-bounded vesicle	9	2.7	1.5	4.3	$3.57 \times 10^{-2}$
	0005815: Microtubule organizing center	7	1.7	1.1	4.8	$3.67 \times 10^{-2}$

Complete data set is given in Supplemental Table S5.

lected six highly expressed genes (Partow et al. 2010) and replaced each ORF with the green fluorescent protein (GFP) (Fig. 6A; Cormack et al. 1997). *TEF1* and *TDH3* were the DSGs isolated in this study. If the overproduction of an unnecessary protein, but not the specific function of the protein, determines the limit of a gene, then the copy number of the artificial gene should also be limited. As shown in Figure 6B, five out of six GFP constructs exhibited significantly lower limits compared with the vector control ( $P < 0.05$ , Student's *t*-test); moreover, the CNLs (the copy

numbers under the  $-Leu-Ura$  condition) of native and GFP replaced genes were highly correlated (Pearson's correlation = 0.90) (Fig. 6C). In addition, acceleration of GFP degradation by adding a degradation signal (Fig. 6A; Jungbluth et al. 2010) further reduced the CNLs (Fig. 6B) and increased the correlation (Pearson's correlation = 0.94) (Fig. 6D), indicating that the accumulated GFP itself does not cause gene toxicity. These observations suggest that a minor increase in the copy number of highly expressed genes causes a protein turnover burden that leads to dosage sensitivity.

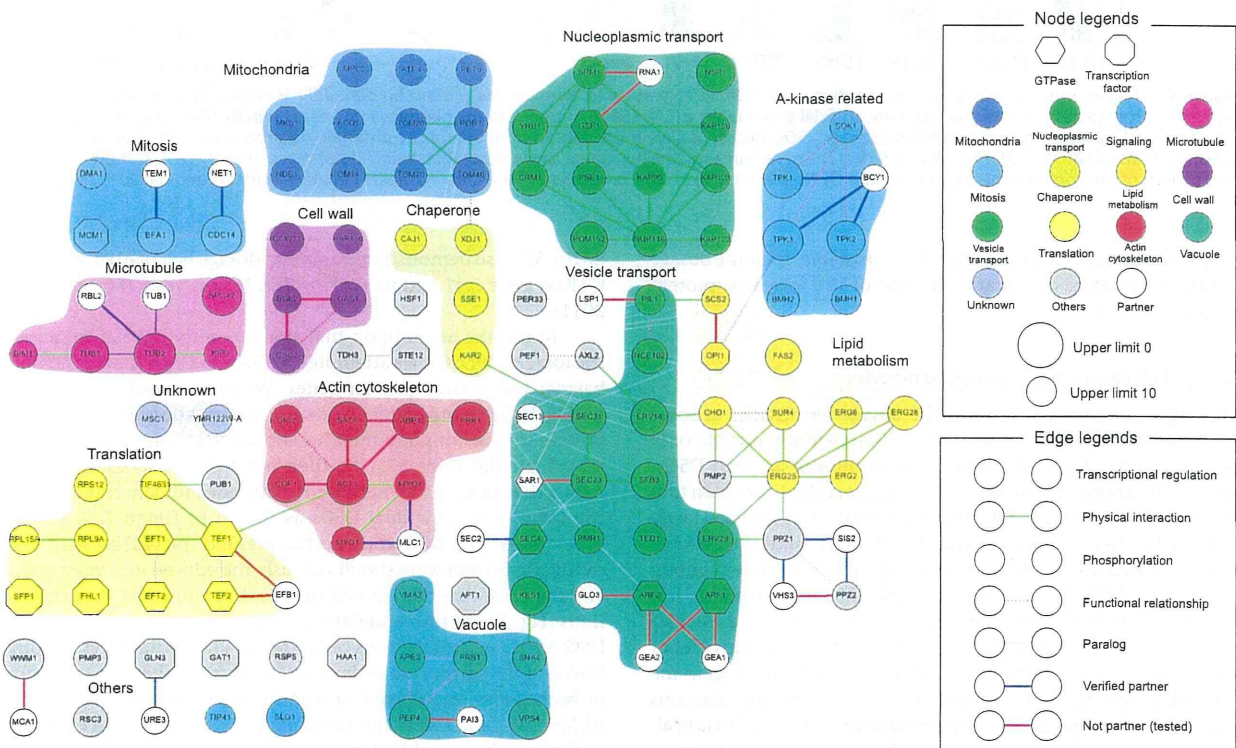


**Figure 5.** Molecular interactions between DSGs. Yeast DSGs were colored according to their functional category annotated in the *Saccharomyces* Genome Database (SGD). Genes were connected by their protein–protein interactions (solid lines), functional relationships (dotted lines), and protein–DNA interactions (thin lines). The interaction data were obtained from BioGRID (<http://thebiogrid.org/>). White-colored genes and bold lines denote the candidate partners and their interactions experimentally tested by 2D-gTOW, respectively (Fig. 7; Supplemental Figs. S11, S12; Table 3; Supplemental Table S7). The network was created using Cytoscape 2.8.1 (<http://www.cytoscape.org/>) and modified using Illustrator CS5 (Adobe) and PowerPoint 2011 (Microsoft).

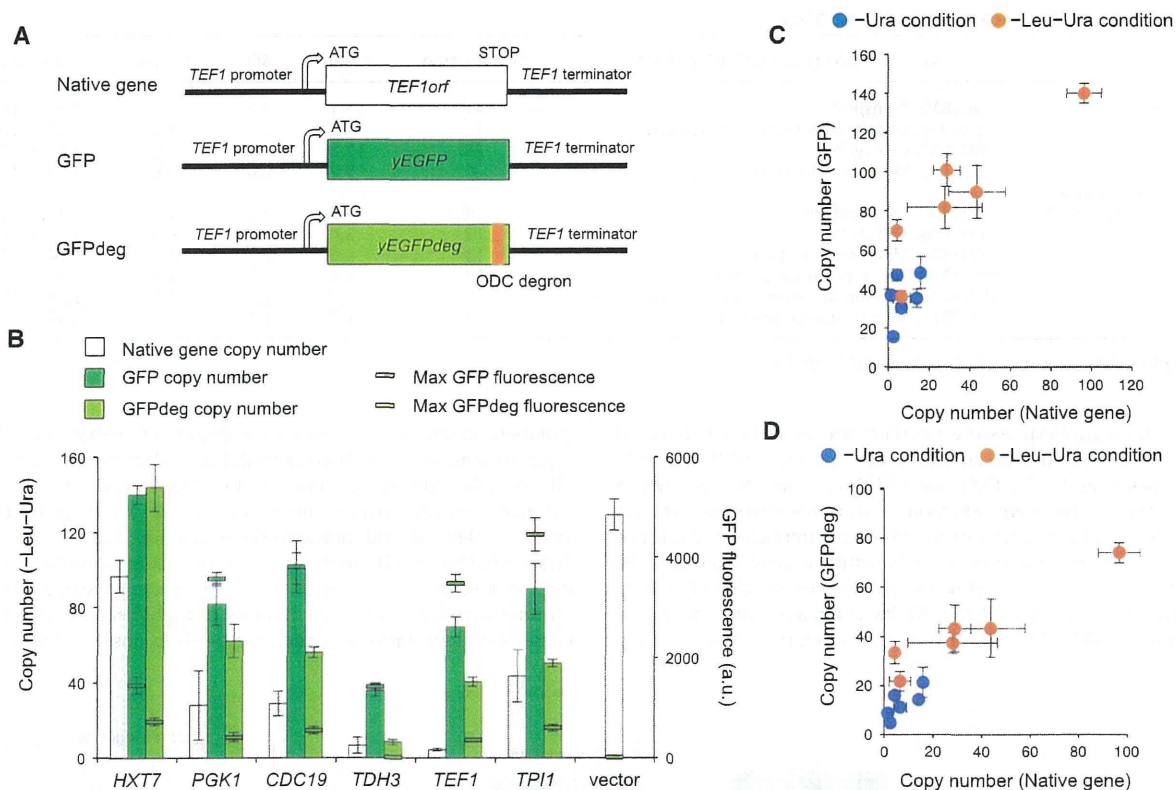


**Figure 6.** Protein burden causes dosage sensitivity. (A) Plasmid constructs to examine the protein burden. *TEF1* is shown as an example of highly expressed target genes. We constructed these artificial genes using pTOW40836, introduced the plasmids into yeast strain BY4741, and then measured the upper CNLs and the maximal GFP fluorescence. ODC degron indicates the degron from the mouse ornithine decarboxylase gene (Jungbluth et al. 2010). (B) CNLs of native and GFP replaced genes. The gene names on the horizontal axis indicate that their ORFs were replaced by GFP, as shown in A. (C) Comparison of the copy numbers of native- and GFP-replaced genes. (D) Comparison of the copy numbers of native- and GFPdeg-replaced genes.

If the protein expressed from the gene is unstable, then the dosage sensitivity could be accelerated because of the increased protein turnover burden.

#### Dosage imbalance causes dosage sensitivity

Although protein burden causes the dosage sensitivities of some DSGs as demonstrated in this study, it is apparently not the only mechanism to explain the dosage sensitivities of all yeast DSGs, because the upper limit of native *TEF1*, e.g., was far lower than that of the GFP construct (Fig. 6B), and some yeast DSGs encoded lowly expressed proteins (Supplemental Fig. S10). As indicated above, protein complex components were highly concentrated among yeast DSGs (Table 1). It is thus possible that stoichiometric imbalance (Papp et al. 2003; Torres et al. 2007; Veitia and Birchler 2010) is another mechanism leading to the dosage sensitivities of yeast DSGs. Ohnologs are genes created by ancient whole-genome duplication events and are retained in the genome. Previous studies and we proposed that they are dosage balanced (Veitia et al. 2008; Makino and McLysaght 2010). Thus, we compared the yeast DSGs and ohnologs and found that they overlapped significantly (Table 1; Supplemental Table S5). This also supports the idea that dosage imbalance causes the dosage sensitivity of DSGs. In fact, we previously demonstrated that the dosage sensitivity of one DSG, *CDC14*, arose from a dosage imbalance against *NET1* (Kaizu et al.

2010). We also demonstrated a similar dosage balance between the GTPase gene *spg1* and its GAP *byr4* in fission yeast (Moriya et al. 2011).

To test the assumption that stoichiometry imbalance causes the toxicity of DSGs, we attempted to identify DSGs that are dosage balanced with their partner genes. We first created a list of potential dosage partners for DSGs using information about protein-protein interactions and their functional effects described in SGD (Supplemental Table S7). We then performed a series of experiments that examined whether the partner candidate could rescue the toxicity of individual DSGs as shown in Figure 7. A gTOW plasmid carrying DSG and another plasmid (pRS423ks) with the candidate partner were simultaneously introduced into yeast cells, and the cells were then grown under -Ura and -Leu-Ura conditions (Fig. 7A). If the candidate is the partner, then the toxicity of DSG is rescued and the cells can grow on -Leu-Ura plates. If both DSG and the partner are in dosage balance, then the copy numbers of both genes in survived cells must be conserved. The case of *GLN3* (DSG) and *URE2* (candidate partner) is shown as an example in Figure 7, B, C, and D. Among the 49 pairs tested, 13 were demonstrated to be in dosage balance (Supplemental Table S7; Supplemental Figs. S11, S12). We note that previously suggested dosage balance between tubulin genes *TUB2* and *TUB1* (Weinstein and Solomon 1990) were hardly detected in our experiment, and we detected the one between *TUB2* and *RBL2* (Supplemental Fig. S13).

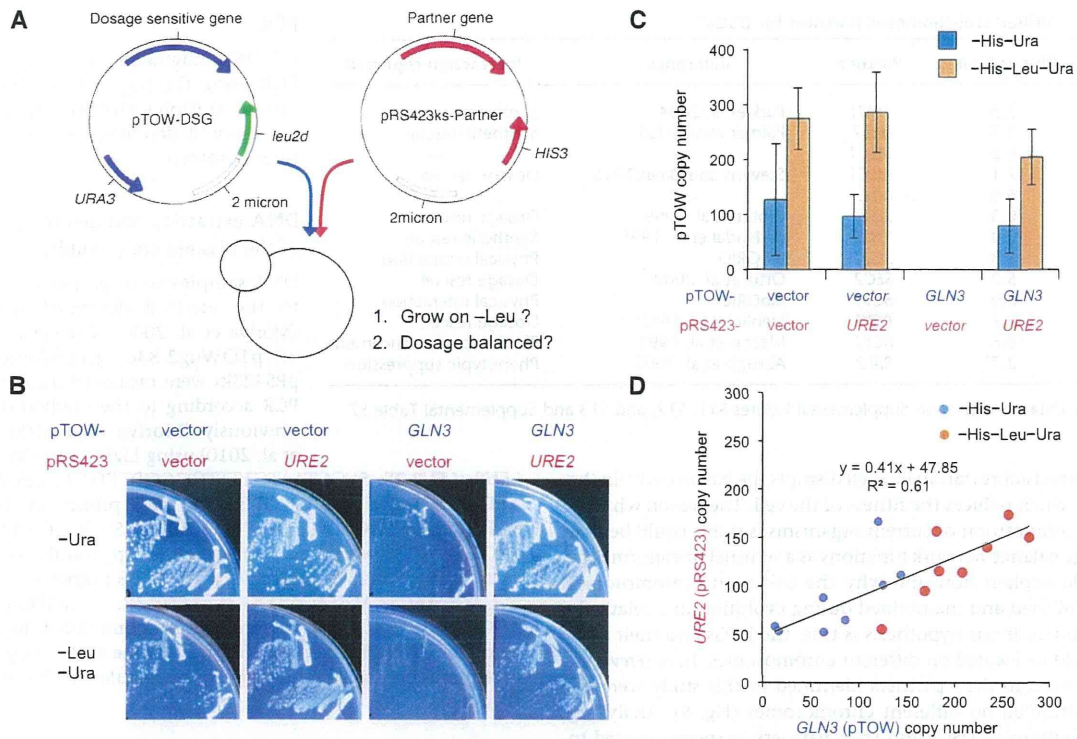


**Figure 7.** Testing dosage balance between DSGs and their candidate partners. (A) The experimental design of 2D-gTOW to determine whether two genes are dosage partners (Kaizu et al. 2010). First, we transformed a yeast strain with two plasmids expressing DSG and its candidate partner and then tested whether the transformant could grow under the  $-Leu$  condition and whether both the plasmids were balanced. (B, C, D) Examples of 2D-gTOW experiments with *GLN3* (DSG) and its partner *URE2*. (B) Plate assay: High copy *URE2* supports the growth of yeast cells with high-copy *GLN3*. (C) Copy numbers of pTOW-*GLN3* and pRS423ks-*URE2* under the low-copy ( $-His-Ura$ ) and high-copy ( $-His-Leu-Ura$ ) conditions. (D) The copy numbers of *GLN3* and *URE2* in 2D-gTOW experiments are balanced. Other experimental results can be found in Supplemental Figures S11, S12, and S13.

Analyzed interactions and confirmed dosage-balanced interactions are indicated by bold lines and blue bold lines in Figure 5, respectively. We thus concluded that dosage imbalance was a cause of the dosage sensitivity of at least some yeast DSGs.

## Discussion

In this study, we applied gTOW to measure the CNLs of overexpression of nearly all protein-coding genes in *S. cerevisiae* and identified 115 DSGs with CNLs of 10 or less. From the characteristics of the genes (e.g., they tended to be highly expressed and complex members), we speculated that protein burden and stoichiometry imbalance caused the dosage sensitivity of these genes. We further experimentally verified the hypothesis using gTOW experiments. The results indicated that there are at least two different causes of dosage sensitivity: specific and nonspecific causes related to gene function. We currently think that for some DSGs, the dosage imbalance by itself causes severe dosage sensitivities. We have isolated some DSGs where the dosage sensitivities were suppressed by the simultaneous overexpressions of their partners (Table 3). The copy numbers of these DSGs can increase (their proteins are further overexpressed) when their partners are abundant, and hence, their protein turnover does not appear to cause their dosage sensitivities.

Disomy of any of the 16 *S. cerevisiae* chromosomes causes cellular growth defects resulting from the overexpression of particular

genes on the disomic chromosome (Torres et al. 2007). Several possible mechanisms by which aneuploidy can cause cellular dysfunction have been proposed (Sheltzer and Amon 2011). Because disomy causes the duplication of all genes on the chromosome, it is difficult to identify specific genes, and consequently the specific mechanisms, causing dosage sensitivity. The mechanisms causing dosage sensitivity that were inspected in this study should have some shared features with aneuploidy.

Although we focused on DSGs in this study, yeast cellular systems were robust against  $\sim 100$ -fold overexpression in  $>80\%$  of their genes (Fig. 2). According to the characteristics of DSGs found in this study, genes with low expression without dosage balance were conversely considered dosage insensitive. Genes with tightly controlled expression or enzymes with regulation that is not subunit dependent (e.g., regulated by intramolecular interactions) will be robust against copy number increase. The domain organization of proteins, e.g., a catalytic domain and a regulatory domain in the same protein, could have evolved to avoid dosage sensitivity.

Why do DSGs remain in the present yeast genome? In addition, why have not cellular systems evolved to avoid the existence of DSGs? One possibility is that dosage sensitivity has its own important function; if DSGs and their dosage partners are reasonably scattered around chromosomal regions, then they will constitute a dosage balance network (the network identified in this study is shown in Fig. 8). This network potentially constrains and secures the composition of an organism's chromosomes because

**Table 3.** Verified stoichiometric partners for DSGs<sup>a</sup>

DSG	Upper limit	Partner	Reference	Interaction reported
<i>BFA1</i>	3.5	<i>TEM1</i>	Park et al. 2004	Synthetic rescue
<i>GLN3</i>	1.5	<i>URE2</i>	Palmer et al. 2009	Synthetic rescue
<i>MYO1</i>	6.5	<i>MLC1</i>	—	—
<i>MYO2</i>	12.1	<i>MLC1</i>	Stevens and Davis 1998	Dosage rescue
<i>MYO4</i>	6.5	<i>MLC1</i>	—	—
<i>PPZ1</i>	0.3	<i>SIS2</i>	Clotet et al. 1999	Dosage rescue
<i>PPZ1</i>	0.3	<i>VHS3</i>	de Nadal et al. 1998	Synthetic rescue
<i>PPZ2</i>	9.3	<i>SIS2</i>	BioGRID	Physical interaction
<i>SEC4</i>	5.2	<i>SEC2</i>	Ortiz et al. 2002	Dosage rescue
<i>TPK1</i>	0.9	<i>BCY1</i>	BioGRID	Physical interaction
<i>TPK2</i>	2.1	<i>BCY1</i>	Nehlin et al. 1992	Dosage rescue
<i>TPK3</i>	0.6	<i>BCY1</i>	Mazón et al. 1993	Phenotypic enhancement
<i>TUB2</i>	2.7 <sup>a</sup>	<i>RBL2</i>	Abruzzi et al. 2002	Phenotypic suppression

<sup>a</sup>Complete data set is given in Supplemental Figures S11, S12, and S13 and Supplemental Table S7.

chromosomal abbreviation in a cell disrupts the balance within the network, which reduces the fitness of the cell. The reason why the genomic composition of current organisms is stable could be that the dosage balance network functions as a sentinel of abnormality. This could explain how and why the eukaryotic chromosomes were established and maintained during evolution in a relatively stable manner. If our hypothesis is true, the DSGs and their partners should be located on different chromosomes. In *S. cerevisiae*, all the DSGs and their partners identified in this study were actually distributed on different chromosomes (Fig. 8). Analyzing the distributions of DSGs and their partners in species related to *S. cerevisiae* (before and after genome duplication) is one way of obtaining further evidence for this hypothesis.

## Methods

### Strains, growth conditions, and yeast transformation

*S. cerevisiae* strain BY4741 (*MATa his3Δ1 leu2Δ0 met15Δ0 ura3Δ0*) (Brachmann et al. 1998) was used for gTOW6000 analysis. Yeast cultivation and transformation were performed as previously described (Amberg et al. 2005). Synthetic complete (SC) medium without indicated amino acids were used for the cultivation of yeast.

### Plasmids used in this study

pTOWug2-836 (Supplemental Fig. S1; Moriya et al. 2012) was used for gTOW6000 analysis. pTOW40836 (a pTOWug2-836 derivative but it does not contain the GFP gene in the backbone) (Moriya et al. 2012), was used for the GFP replacement experiments in Figure 6. pRS423ks, which was used to clone partner genes for two-dimensional gTOW experiments, is a derivative of pRS423 (Christianson et al. 1992), and it has two additional primer sites outside the multicloning site (indicated as K\_primer and S\_primer in Supplemental Fig. S14). The K and S priming sites allowed us to selectively amplify the insert of pRS423ks from the cells harboring pTOW and pRS423ks. gTOW6000 plasmid clones were constructed as described below. The plasmids used for the frameshift analysis, the segmentation analysis, and the GFP replacement analysis were constructed as shown in Supplemental Figures S15, S16, and S17, respectively. Primer sequences used to construct the gTOW6000 plasmids are listed in Supplemental Table S8. Other primer sequences are available upon request. Individual plasmid in gTOW6000 is available from National BioResource Project-Yeast (<http://yeast.lab.nig.ac.jp/>).

### PCR

All DNA fragments were amplified by PCR using the high-fidelity DNA polymerase KODplus (Toyobo) according to the method described in the manufacturer's protocol.

### DNA extraction and determination of the plasmid copy number

DNA samples were prepared according to the method described previously (Moriya et al. 2006). The copy numbers of pTOWug2-836, pTOW40836 and pRS423ks were measured using real-time PCR according to the method described previously (Moriya et al. 2006; Kaizu et al. 2010) using Lightcycler480 (Roche).

*LEU2* (*LEU2*-2F: 5'-GCTAATGTTTTGGCCTCTTC-3'; *LEU2*-2R: 5'-ATTAGGTGGGTTGGGTTCT-3') and *HIS3* primer sets (*HIS3*-1F: 5'-TTCCGGCTGTCGCTAAT-3'; *HIS3*-1R: 5'-GCGCAAATCCTGATCCAAAC-3') were used to measure the copy numbers of pTOW vectors and pRS423ks, respectively. The *LEU3* primer set (*LEU3*-3F: 5'-CAGCAACTAAGGACAAGG-3'; *LEU3*-3R: 5'-GGTCGTTAATGAGCTCC-3') was used to amplify the genomic DNA. Because we used *LEU3* as a reference gene for the genome in the copy number determination using real-time PCR, the calculated CNL of *LEU3* is always one.

### Measuring GFP fluorescence

GFP fluorescence of cell culture was measured using Infinite F200 microplate reader (TECAN)

### Construction of gTOW6000 clones and the analysis

The entire scheme of gTOW6000 analysis is shown in Figure 1. The gTOW6000 analysis was separated into eight steps as follows.

#### *Design primers to amplify each target gene (step 1), and amplify the target genes using PCR (step 2)*

In this study, we attempted to analyze all protein-coding genes on the *S. cerevisiae* chromosome. To clone all genes with their regulatory regions for "Characterized" and "Uncharacterized" ORFs, we amplified a DNA fragment containing each target ORF with upstream and downstream regions spanning the neighboring ORFs. We ignored "Dubious ORF," autonomous replicating sequence (ARS), and other RNA elements. Supplemental Figure S2A presents an example of the analysis. Each region shown in blue was cloned into individual pTOW plasmids. It is thus possible that the plasmid CNL is determined by the effect of non-ORF elements within each clone instead of the cloned protein-coding genes. This possibility will be solved using a frameshift mutation analysis, as described in another section. Supplemental Figure S2B shows the design of the primers used to amplify the regions containing target genes by PCR. The primers consist of 23-bp priming sequences of the neighboring ORFs and 25-bp adaptor sequences of the vector for gap-repair cloning. The adaptor sequences of the up primer and the down primer were 5'-cggcgcctagaactagtGGATCC...-3' and 5'-attgggtaccggccccccCTCGAG...-3', respectively. The sequences shown in capital letters in the up and down primer sequences are the BamHI and XhoI sites, respectively. The primer sequences of pTOWug2-836 are shown in Supplemental Figure S1B. According to the annotation of SGD (released on July 28, 2007), primers for

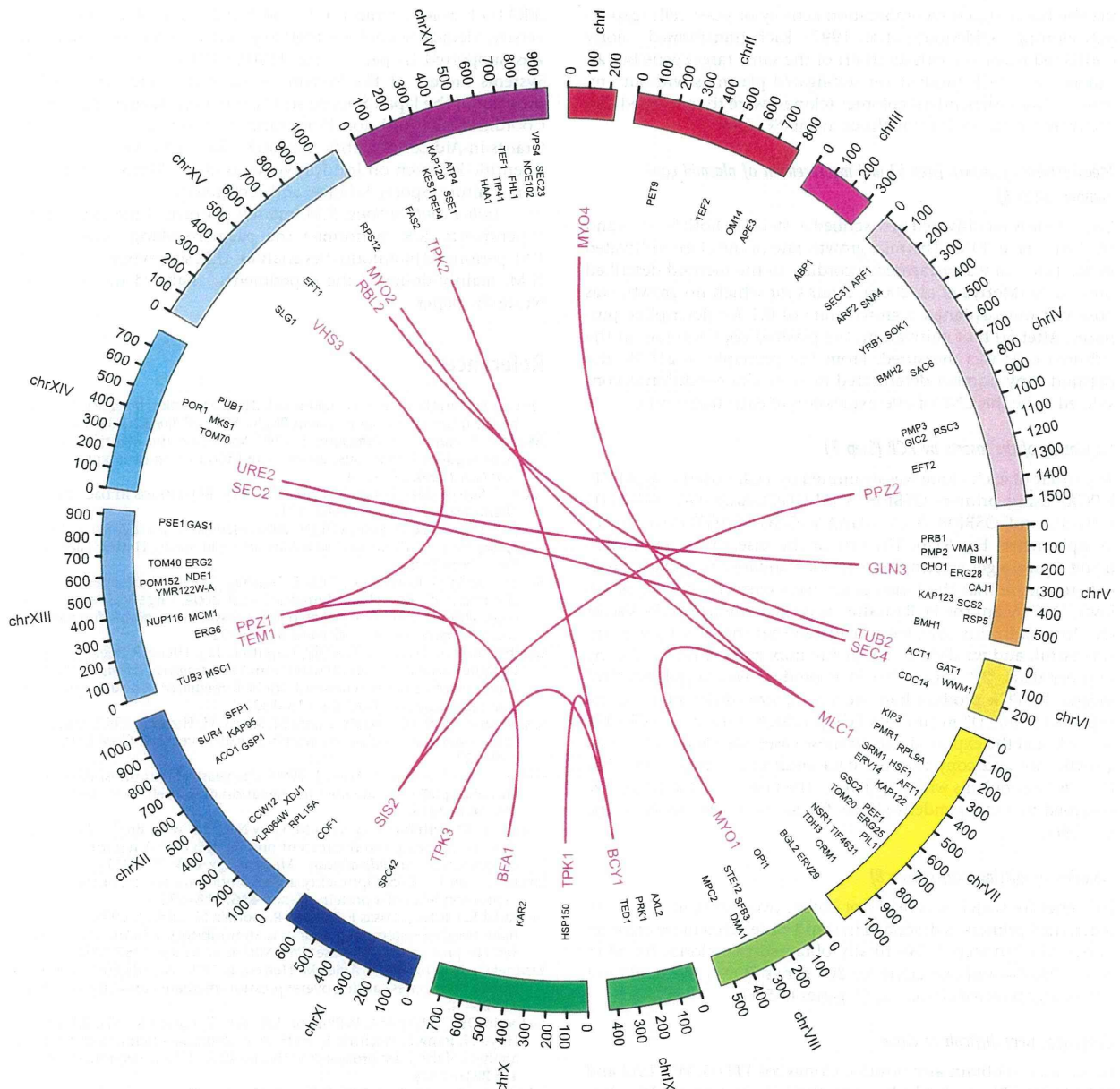


**Figure 8.** Intrachromosomal interactions connected with DSGs and their partner genes. Locations of DSGs and their partner genes and their interactions identified in this study are visualized using Circos software (Krzywinski et al. 2009). The locations of 115 yeast DSGs are also shown.

amplifying 5806 genes were designed using a Perl script. Each gene was amplified by PCR using each primer set and the BY4741 genome as a template (first PCR). Via PCR, 98.4% of the obtained PCR products had the correct size. For the genes for which we could not obtain PCR products, we redesigned the primers. If the distance to the neighboring gene was too large, then we shortened the length of the noncoding region to 1 kb. If the target ORF was too large, we designed primers as listed in Supplemental Table S9 to amplify segments of the gene and connected the segments by gap repair (see below). We thus redesigned primers for 90 genes. The primer sets for genes next to each of the 16 centromeres were first designed to

ensure that the amplified fragments contain the centromeres. As expected, all 32 of the DNA fragments containing centromeres expressed one copy of the gTOW plasmid per cell (data not shown). We thus redesigned primers to remove the centromeres.

#### *Transformation (gap-repair cloning; step 3) and selecting two independent clones for each gene (step 4)*

The PCR products amplified using the aforementioned primers and pTOWug2-836 digested with BamHI and XhoI were simultaneously introduced into BY4741 yeast cells. Each gene was inserted



via the homologous recombination activity of yeast cells (gap-repair cloning) (Oldenburg et al. 1997). Each transformed colony contained plasmids with an insert of the same target gene but an independent PCR product (or self-ligated plasmids without any insert). Two independent colonies (clones) were thus selected and cultivated in SC medium without uracil (SC-Ura).

#### Measurement of growth (step 5) and measurement of plasmid copy numbers (step 6)

Each clone was cultivated as described in step 4 in both SC-Ura and SC-Leu-Ura at 30°C. The max growth rate of the clone cultivated in SC-Leu-Ura was measured according to the method described previously (Moriya et al. 2006). Strains for which no growth was observed were assigned a growth rate of 0.1 for descriptive purposes. After 50 h of cultivation, the plasmid copy number in the cultured cells was measured. From the principle of gTOW, the plasmid copy number determined in -Leu-Ura condition is considered to be the CNL of overexpression of each target gene.

#### Validation of the inserts by PCR (Step 7)

The insert of each clone was examined by PCR (insert-check PCR; icPCR) using primers OSBI0873 (5'-GGCGAAGGGGATGTGCTG-3') and OSBI0870 (5'-GGAAAGCGGCAGTGAGCGC-3') (Supplemental Fig. S1B). The size of the insert was determined using Agarose gel electrophoresis. We validated the icPCR products to ensure that the target genes were correctly cloned as follows: "NI" meant the PCR product was the same size as the vector (No-Insert). In this case, we considered that the cloning was unsuccessful, and we did not adopt the max growth rate and copy number data. "N" meant No PCR product was amplified. "W" meant the PCR product had the wrong size (different from the expected size). "D" meant two PCR products were amplified. One of them had the expected size. In these cases, we adopted the max growth rate and copy number data because it was possible that there were problems with icPCR (e.g., the target was too large). We obtained two independent clones for 88.9% of the genes in the first cycle.

#### Isolation of missing clones (step 8)

For genes for which we could not obtain two clones in step 7, we redesigned primers as described in step 1 or selected more colonies as described in step 4. We finally obtained two clones for 5548 genes (95.6%) and one clone for 203 genes (3.5%). We could not obtain any positive clones for 55 genes (5.5%).

#### Genes that were difficult to clone

We could not obtain any positive clones for *YFL037W/TUB2* and *YFL039C/ACT1*, probably because they are too toxic. We thus made plasmids with those genes in *Escherichia coli* and confirmed that they were too toxic for the transformants to form colonies (data not shown). We thus concluded that they were very low limit genes. In addition, for *TUB2*, we created a promoter-deletion series and obtained a *TUB2* allele with a 100-bp promoter (*tub2d-100*, its CNL was 2.7). We thus used these data for *TUB2*. As mentioned above, we could not obtain any clones for 55 genes. Approximately half of them were retrotransposons and helicases encoded near telomeres.

#### Acknowledgments

We thank Yuki Shimizu-Yoshida (Sony CSL), Kazunari Kaizu (Riken), Ayako Chino, and Masataka Sasabe (Okayama University) for valuable discussions about this work, and Naomi Fujimoto

(ERATO Kawaoka Project, JST) and Kazuko Matsubara (Keio University, Medical School) for their experimental support. This work was supported in part by the ERATO-SORST Kitano Symbiotic Systems Project of the Systems Biology Institute, the PRESTO program of the Japan Science and Technology Agency, the Special Coordination Fund for Promoting Sciences and Technology, Grants-in-Aid for Scientific Research (B), and Grants-in-Aid for Scientific Research on Innovative Areas of the Ministry of Education, Culture, Sports, Science, and Technology.

**Author contributions:** K.M. mainly performed the gTOW6000 experiments. R.K. performed the partner-seeking experiments. T.M. performed bioinformatics analysis. H.K. supervised the project. H.M. mainly designed the experiments, analyzed the data, and wrote the paper.

#### References

- Abruzzi KC, Smith A, Chen W, Solomon F. 2002. Protection from free  $\beta$ -tubulin by the  $\beta$ -tubulin binding protein Rbl2p. *Mol Cell Biol* **22**: 138–147.
- Akada R, Yamamoto J, Yamashita I. 1997. Screening and identification of yeast sequences that cause growth inhibition when overexpressed. *Mol Gen Genet* **254**: 267–274.
- Alon U, Surette MG, Barkai N, Leibler S. 1999. Robustness in bacterial chemotaxis. *Nature* **397**: 168–171.
- Amberg DC, Burke D, Strathern JN. 2005. *Methods in yeast genetics: A Cold Spring Harbor Laboratory Course Manual*. Cold Spring Harbor Laboratory Press, New York.
- Boyer J, Badis G, Fairhead C, Talla E, Hantraye F, Fabre E, Fischer G, Hennequin C, Koszul R, Lafontaine I, et al. 2004. Large-scale exploration of growth inhibition caused by overexpression of genomic fragments in *Saccharomyces cerevisiae*. *Genome Biol* **5**: R72.
- Brachmann CB, Davies A, Cost GJ, Caputo E, Li J, Hieter P, Boeke JD. 1998. Designer deletion strains derived from *Saccharomyces cerevisiae* S288C: A useful set of strains and plasmids for PCR-mediated gene disruption and other applications. *Yeast* **14**: 115–132.
- Christianson TW, Sikorski RS, Dante M, Shero JH, Hieter P. 1992. Multifunctional yeast high-copy-number shuttle vectors. *Gene* **110**: 119–122.
- Clotet J, Garí E, Aldea M, Ariño J. 1999. The yeast ser/thr phosphatases sit4 and ppz1 play opposite roles in regulation of the cell cycle. *Mol Cell Biol* **19**: 2408–2415.
- Cormack BP, Bertram G, Egerton M, Gow NA, Falkow S, Brown AJ. 1997. Yeast-enhanced green fluorescent protein (yEGFP): A reporter of gene expression in *Candida albicans*. *Microbiology* **143**: 303–311.
- Dekel E, Alon U. 2005. Optimality and evolutionary tuning of the expression level of a protein. *Nature* **436**: 588–592.
- de Nadal E, Clotet J, Posas F, Serrano R, Gomez N, Ariño J. 1998. The yeast halotolerance determinant Hal3p is an inhibitory subunit of the Ppz1p Ser/Thr protein phosphatase. *Proc Natl Acad Sci* **95**: 7357–7362.
- Espinete C, de la Torre MA, Aldea M, Herrero E. 1995. An efficient method to isolate yeast genes causing overexpression-mediated growth arrest. *Yeast* **11**: 25–32.
- Gelperin DM, White MA, Wilkinson ML, Kon Y, Kung LA, Wise KJ, Lopez-Hoyo N, Jiang L, Piccirillo S, Yu H, et al. 2005. Biochemical and genetic analysis of the yeast proteome with a movable ORF collection. *Genes Dev* **19**: 2816–2826.
- Ghaemmaghami S, Huh WK, Bower K, Howson RW, Belle A, Dephoure N, O'Shea EK, Weissman JS. 2003. Global analysis of protein expression in yeast. *Nature* **425**: 737–741.
- Jones GM, Stalker J, Humphray S, West A, Cox T, Rogers J, Dunham I, Prelich G. 2008. A systematic library for comprehensive overexpression screens in *Saccharomyces cerevisiae*. *Nat Methods* **5**: 239–241.
- Jungbluth M, Renicke C, Taxis C. 2010. Targeted protein depletion in *Saccharomyces cerevisiae* by activation of a bidirectional degron. *BMC Syst Biol* **4**: 176.
- Kaizu K, Moriya H, Kitano H. 2010. Fragilities caused by dosage imbalance in regulation of the budding yeast cell cycle. *PLoS Genet* **6**: e1000919.
- Krantz M, Ahmadpour D, Ottosson LG, Warringer J, Waltermann C, Nordlander B, Klipp E, Blomberg A, Hohmann S, Kitano H. 2009. Robustness and fragility in the yeast high osmolarity glycerol (HOG) signal-transduction pathway. *Mol Syst Biol* **5**: 281.
- Krzywinski M, Schein J, Birol I, Connors J, Gascoyne R, Horsman D, Jones SJ, Marra MA. 2009. CircoS: An information aesthetic for comparative genomics. *Genome Res* **19**: 1639–1645.
- Little JW, Shepley DP, Wert DW. 1999. Robustness of a gene regulatory circuit. *EMBO J* **18**: 4299–4307.

- Liu H, Krizek J, Bretscher A. 1992. Construction of a GAL1-regulated yeast cDNA expression library and its application to the identification of genes whose overexpression causes lethality in yeast. *Genetics* **132**: 665–673.
- Makino T, McLysaght A. 2010. Ohnologs in the human genome are dosage balanced and frequently associated with disease. *Proc Natl Acad Sci* **107**: 9270–9274.
- Mazón MJ, Behrens MM, Morgado E, Portillo F. 1993. Low activity of the yeast cAMP-dependent protein kinase catalytic subunit Tpk3 is due to the poor expression of the TPK3 gene. *Eur J Biochem* **213**: 501–506.
- Moriya H, Shimizu-Yoshida Y, Kitano H. 2006. In vivo robustness analysis of cell division cycle genes in *Saccharomyces cerevisiae*. *PLoS Genet* **2**: e111.
- Moriya H, Chino A, Kapuy O, Csikász-Nagy A, Novák B. 2011. Overexpression limits of fission yeast cell-cycle regulators in vivo and in silico. *Mol Syst Biol* **7**: 556.
- Moriya H, Makanae K, Watanabe K, Chino A, Shimizu-Yoshida Y. 2012. Robustness analysis of cellular systems using the genetic tug-of-war method. *Mol Biosyst* **8**: 2513–2522.
- Nehlin JO, Carlberg M, Ronne H. 1992. Yeast SKO1 gene encodes a bZIP protein that binds to the CRE motif and acts as a repressor of transcription. *Nucleic Acids Res* **20**: 5271–5278.
- Niu W, Li Z, Zhan W, Iyer VR, Marcotte EM. 2008. Mechanisms of cell cycle control revealed by a systematic and quantitative overexpression screen in *S. cerevisiae*. *PLoS Genet* **4**: e1000120.
- Oldenburg KR, Vo KT, Michaelis S, Paddon C. 1997. Recombination-mediated PCR-directed plasmid construction in vivo in yeast. *Nucleic Acids Res* **25**: 451–452.
- Ortiz D, Medkova M, Walch-Solimena C, Novick P. 2002. Ypt32 recruits the Sec4p guanine nucleotide exchange factor, Sec2p, to secretory vesicles; evidence for a Rab cascade in yeast. *J Cell Biol* **157**: 1005–1015.
- Palmer LK, Baptiste BA, Fester JC, Perkins JC, Keil RL. 2009. RRD1, a component of the TORC1 signalling pathway, affects anaesthetic response in *Saccharomyces cerevisiae*. *Yeast* **26**: 655–661.
- Papp B, Pál C, Hurst LD. 2003. Dosage sensitivity and the evolution of gene families in yeast. *Nature* **424**: 194–197.
- Park JE, Park CJ, Sakchaisri K, Karpova T, Asano S, McNally J, Sunwoo Y, Leem SH, Lee KS. 2004. Novel functional dissection of the localization-specific roles of budding yeast polo kinase Cdc5p. *Mol Cell Biol* **24**: 9873–9886.
- Partow S, Siewers V, Bjørn S, Nielsen J, Maury J. 2010. Characterization of different promoters for designing a new expression vector in *Saccharomyces cerevisiae*. *Yeast* **27**: 955–964.
- Sheltzer JM, Amon A. 2011. The aneuploidy paradox: Costs and benefits of an incorrect karyotype. *Trends Genet* **27**: 446–453.
- Sopko R, Huang D, Preston N, Chua G, Papp B, Kafadar K, Snyder M, Oliver SG, Cyert M, Hughes TR, et al. 2006. Mapping pathways and phenotypes by systematic gene overexpression. *Mol Cell* **21**: 319–330.
- Stevens RC, Davis TN. 1998. Mlc1p is a light chain for the unconventional myosin Myo2p in *Saccharomyces cerevisiae*. *J Cell Biol* **142**: 711–722.
- Stevenson LE, Kennedy BK, Harlow E. 2001. A large-scale overexpression screen in *Saccharomyces cerevisiae* identifies previously uncharacterized cell cycle genes. *Proc Natl Acad Sci* **98**: 3946–3951.
- Stoebel DM, Dean AM, Dykhuizen DE. 2008. The cost of expression of *Escherichia coli* lac operon proteins is in the process, not in the products. *Genetics* **178**: 1653–1660.
- Torres EM, Sokolsky T, Tucker CM, Chan LY, Boselli M, Dunham MJ, Amon A. 2007. Effects of aneuploidy on cellular physiology and cell division in haploid yeast. *Science* **317**: 916–924.
- Vavouri T, Semple JI, Garcia-Verdugo R, Lehner B. 2009. Intrinsic protein disorder and interaction promiscuity are widely associated with dosage sensitivity. *Cell* **138**: 198–208.
- Veitia RA, Birchler JA. 2010. Dominance and gene dosage balance in health and disease: Why levels matter! *J Pathol* **220**: 174–185.
- Veitia RA, Bottani S, Birchler JA. 2008. Cellular reactions to gene dosage imbalance: Genomic, transcriptomic and proteomic effects. *Trends Genet* **24**: 390–397.
- von Dassow G, Meir E, Munro EM, Odell GM. 2000. The segment polarity network is a robust developmental module. *Nature* **406**: 188–192.
- Wagner A. 2005. Energy constraints on the evolution of gene expression. *Mol Biol Evol* **22**: 1365–1374.
- Weinstein B, Solomon F. 1990. Phenotypic consequences of tubulin overproduction in *Saccharomyces cerevisiae*: Differences between  $\alpha$ -tubulin and  $\beta$ -tubulin. *Mol Cell Biol* **10**: 5295–5304.
- Yoshikawa K, Tanaka T, Ida Y, Furusawa C, Hirasawa T, Shimizu H. 2011. Comprehensive phenotypic analysis of single-gene deletion and overexpression strains of *Saccharomyces cerevisiae*. *Yeast* **28**: 349–361.
- Zaslaver A, Mayo AE, Rosenberg R, Bashkin P, Sberro H, Tsalyuk M, Surette MG, Alon U. 2004. Just-in-time transcription program in metabolic pathways. *Nat Genet* **36**: 486–491.

Received July 25, 2012; accepted in revised form October 22, 2012.